THE AMERICAN SOCIETY OF MECHANICAL ENGINEERS
345 E. 47th St., New York, N.Y. 10017

98-GT-110

HEAT TRANSFER AND PRESSURE DROP IN PIN-FIN TRAPEZOIDAL DUCTS

J.-J. HWANG D.-Y. LIA Y.-P. TSIA
Department of Mechanical Engineering
Chung-Hua University
Hsinchu, Taiwan 300, ROC
Phone : 886-35374281, Fax : 886-35373771, Email : jjhwang@chu.edu.tw

ABSTRACT

Experiments are conducted to determine the log-mean averaged Nusselt number and overall pressure-drop coefficient in a pin-fin trapezoidal duct that models the cooling passages in modern gas turbine blades. The effects of pin arrangement (in-line and staggered), flow Reynolds number ($6.000 \leqq Re \leqq 40.000$) and ratio of lateral-to-total flow rate ($0 \leqq \varepsilon \leqq 1.0$) are examined. The results of smooth trapezoidal ducts without pin arrays are also obtained for comparison. It is found that, for the single-outlet-flow duct, the log-mean averaged Nusselt number in the pin-fin trapezoidal duct with lateral outlet is insensitive to the pin arrangement, which is higher than that in straight-outlet-flow duct with the corresponding pin array. As for the trapezoidal ducts having both outlets, the log-mean averaged Nusselt number has a local minimum value at about $\varepsilon = 0.3$. After about $\varepsilon \geqq 0.8$, the log-mean averaged Nusselt number is nearly independent on the pin configuration. Moreover, the staggered pin array pays more pressure-drop penalty as compared with the in-line pin array in the straight-outlet-flow duct; however, in the lateral-outlet-flow duct, the in-line and staggered pin arrays yield almost the same overall pressure drop.

NOMENCLATURE

A total heat transfer area, including the end walls and the pin surfaces [m^2]
A_c cross sectional area at the test section inlet [m^2]
A_l cross section area at lateral outlet [m^2]
AR aspect ratio the rectangular duct
c_p specific heat at constant pressure [kJ/kg-K]
De equivalent hydraulic diameter at the trapezoidal duct inlet, i.e., $4A_c/(2W+H_1+H_2)$ [m]
d pin diameter [m]
f Darcy friction factor
G total mass flux [kg/m^2-s]
G_l mass flux in the lateral duct [kg/m^2-s]
H_1 height of the longer side wall of the trapezoidal duct [m]
H_2 height of the short side wall of the trapezoidal duct [m]
K_L pressure-drop coefficient, $2 \Delta P/(G^2/\rho)$
k_f air thermal conductivity [W/m-K]
L trapezoidal duct length along streamwise direction, [m]
l fin length (or height) [m]
$\overline{Nu}$ log-mean averaged Nusselt number, $Q_c \bullet De/(A \bullet \Delta T_{lm} \bullet k_f)$
$\overline{Nu_s}$ log-mean averaged Nusselt number for the developing smooth trapezoidal duct
Pr Prandtl number
ΔP pressure drop across the test section [kPa]
Q_c net convective heat from the test section to the coolan [W]
Q_e electrical power dissipated by the foil heater [W]
Q_l total heat losses from the test section [W]
Re Reynolds number, $G \bullet De / \mu$
S_L longitude spacing between the pins [m]
S_T transverse spacing between the pins [m]
T_{bi} air bulk mean temperature at the test section inlet [K]
T_{bl} bulk mean temperature of air at the lateral exit [K]
T_{bo} average bulk mean temperature of air at the test section exits [K]
T_{bs} bulk mean temperature of air at the straight exit [K]
$\overline{T}_w$ average temperature on the end wall [K]
ΔT_{lm} log-mean temperature difference, Eq. (3) [K]
W width of the heated plate, Fig. 3 [m]

Greek Symbols

ε ratio of lateral-to-total flow rate, i.e., $G_l A_l / G A_c$
ρ air density [kg/m^3]

Presented at the International Gas Turbine & Aeroengine Congress & Exhibition
Stockholm, Sweden — June 2–June 5, 1998
This paper has been accepted for publication in the Transactions of the ASME
Discussion of it will be accepted at ASME Headquarters until September 30, 1998

μ viscosity of the air [kg/s-m^2]

Subscripts

b bulk mean
c cross section or convection
l lateral or loss
s smooth or straight
w wall

INTRODUCTION

It is well known that the gas turbine thermal efficiency can be improved by increasing the turbine inlet gas temperature, which unavoidably will increase the heat load to the turbine components. Therefore, highly sophisticated internal and external cooling techniques for turbine blades have been developed over the years in order to maintain an acceptable safety requirement below the extreme operating conditions. This study focuses on the internal cooling channels at the trailing edge of turbine blade. Figure 1 shows a crosscut view of an advanced gas turbine blade. In the trailing edge region of blade, aerodynamic considerations demand a small wedge angle for the blade profile. As a result, the internal cooling passages become so narrow that the choice of the cooling method is limited. Pin fins are one augmentation device that can be used to increase heat transfer in this region. The pin fins of circular cross section span the distance between the suction and pressure surfaces that form the endwalls of the cooling passage. Some of the coolant from the blade base exits through bleed slots at the blade tip; the remainder passes through the pin-fin channel and then is ejected from the slots along the trailing edge of the airfoil. Heat from the hot gas stream is convected from not only the endwalls but also the pin-fin surfaces. Also, the pin fins promote turbulence that enhances heat transfer.

VanFossen (1982) measured the overall heat transfer coefficients in large aspect-ratio rectangular ducts (AR = 10, and 20) with staggered arrays of short pin fins ($0.5 < l/d < 2.0$). Heat transfer rates were averaged over the four-row pin array. It was found that the overall heat transfer coefficients for short pins were lower than those for long pin fins (l/d = 8.0). Then, by using the same flow path as that in VanFossen (1982), Brigham and VanFossen (1984) investigated the effects of the pin row number in streamwise direction and pin length (height) on the array-averaged heat transfer. Results showed that the array-averaged heat transfer coefficients for the eight-row configuration were slightly higher than those for the four-row configuration. In addition, for an l/d less than 2, the array-averaged heat transfer was not affected by the pin length; while, as $l/d > 2$, the heat transfer increased significantly with an increase of l/d.

Metzger et al. (1982) studied experimentally the local heat transfer variation in a rectangular duct (AR =10) with staggered short pin array (l/d = 1.0). Results showed that the local heat transfer increased in the first few rows, reached a peak value and then slowly decreased to a fully developed value. The overall heat transfer correlations were also developed in their work in terms of the Reynolds number for two pin configurations (i.e., $S_T/d = S_L/d = 2.5$, and $S_T/d = 2.5$, and $S_L/d = 1.5$). Later, Metzger and Haley (1982) conducted experiments to examine the effect of replacing the thermally active (copper) pins with the thermally non-active (wooden) pins on the heat transfer in rectangular ducts (AR =10) with a staggered pin array. It was found that the streamwise development of the row-averaged Nusselt number in these two kinds of pins showed the same rapidly increasing then gradually decreasing trend. The overall heat transfer in the copper-pin case was higher than that in the wooden-pin case at high Reynolds numbers but was lower at low Reynolds numbers. Metzger et al. (1984) further experimentally investigated the effect of varying the orientation of flattened pins with respect to the main flow direction on the heat transfer and pressure drops in pin-fin rectangular channels. They found that, by varying the orientation of the pin-fin array, it was possible to increase the heat transfer and, in the mean time, reduce the pressure drop. Moreover, the use of flattened pins increased the heat transfer slightly but doubled the pressure loss.

Lau et al. (1987) employed the naphthalene sublimation technique to measure the distributions of local endwall heat transfer coefficient in rectangular channels (AR = 10) with in-line and staggered pin-fin arrays. The effects of Reynolds number, pin configuration, and entrance length on the local endwall heat transfer coefficient distribution were examined. Overall, and row-averaged Nusselt numbers were compared well with the previous published data (Metzger et al., 1982). Lau et al. (1989) further experimentally studied the overall heat transfer and friction factor in pin-fin rectangular channels (AR = 10) with lateral ejection. It was found that the overall heat transfer for a rectangular pin-fin channel with lateral ejection was lower than that for a rectangular channel with no ejection holes.

As noted in the above discussion, the available data concerning the pin-fin heat transfer in open literature is mostly for ***rectangular*** channels with or without lateral ejection. As detailed by the external shape of the blade trailing edges (Fig. 1), however, the cooling cavities in this region often have very a narrow ***trapezoidal*** shape with characteristically small passage aspect ratios. In this circumstance, the pin fins spanning the distance between two principal walls of the trapezoidal passage have different lengths. The heat transfer and friction characteristics in such a kind of channel, especially with lateral outlet flow, should be different from those in rectangular channels. However, to the author's best knowledge, the related studies so far have not considered the overall heat transfer and pressure-drop characteristics in pin-fin trapezoidal ducts. Therefore, the present study experimentally investigates the overall heat transfer and pressure drop in pin-fin trapezoidal ducts with straight and / or lateral outlets. During this work, the log-mean averaged heat transfer and overall pressure drop across the pin-fin duct are obtained for various pin configurations (in-line and staggered), ratios of lateral-to-total flow rate ($0 \leqq \varepsilon \leqq 1.0$), and Reynolds numbers ($6.000 \leqq Re \leqq 40.000$) typical of gas turbine airfoil application.

EXPERIMENTAL APPARATUS

Figure 2 shows schematically the layout of experimental apparatus and the detailed construction of the test section. Air from the laboratory room flows through a honeycomb straightener, a bell-mouth inlet, the entrance (unheated) section, and then into the test section. Subsequently, a part of air is drawn laterally by a 3 hp blower; the remainder traverses the test section, then exits through the straight

outlet, and is finally pulled downstream by another blower (5 hp). Both streams exit to the outside of building via an exhaust system. The lateral and straight flow rates are controlled by varying the motor speed of the blowers via PWM (Pulse Wave Modulation) inverters, and are measured by the rotameters (with an accuracy of 5 %) situated at the downstream of the lateral and straight exits.

The test section is a wide symmetric trapezoidal duct with a array of various-length pin fins that models the pin-fin cooling passage in a gas turbine blade. As shown in Fig. 2, the upper and lower walls (i.e., the endwalls) of the test section are heat transfer surfaces; while the left (long) side wall is adiabatic. The right (short) side wall of the test section is either blocked or open depending the test conditions. The heat transfer surface having area of 160 by 160 mm^2 ($W \times L$, Fig. 3 (a)) is constructed of a 5-mm thick aluminum plate associated with a 0.18 mm-thick foil heater. The foil heater is flatly and uniformly adhered on the backside surface of the aluminum plate by using thermal epoxy to ensure good contact. The heated aluminum plate is then mounted flush on a 10-mm thick bakelite holder. The longer (left) channel side wall of 40-mm in height (H_l, Fig. 3(a)) is machined from a 10-mm thick bakelite plate which is held in place by bolts extending through two principal walls and bakelite material. The blockages for the straight and lateral exits are made of balsa wood. These blockages are not attached permanently to the test section. Rather, they are screwed in place from the top and bottom channel walls. The assembly is sealed from air leakage with petrolatum sealant. All outer surfaces of the test section are well surrounded by the glassfiber to prevent the possible heat losses. Twenty-five (5 by 5) aluminum pins with diameter of 12 mm (d) are well fitted between two heated walls with thermal epoxy in a required arrangement. The aluminum pins adopted are because of their high conductivity and machinability. The length of the aluminum pins varies from $1.3 \leqq l/d \leqq 3.6$ depending the location within the trapezoidal duct. The pin spacings both in the longitude (S_L) and in the transverse (S_T) directions are fixed 30 mm (Fig. 3(a)). Note that the thickness of epoxy used at each of the above-mentioned interfaces is less than 0.12 mm. The heat transfer flux to the portion of plate under the pin is reduced by less than 2%; thus the thermal resistance of the epoxy is negligible (Hwang, 1997).

As shown in Fig. 2, fourteen copper-constantan thermocouples are distributed over the heated plate for wall temperature measurements. The junction-beads of thermocouple (about 0.15-mm in diameter) are carefully embedded in the wall, and then ground flat to ensure that they are flush with the surface. Additional seven thermocouples (one at the duct inlet, three at the straight outlet, and three at the lateral outlet, respectively) are used to measure the air temperature. All temperature signals are first sent to a hybrid recorder (YOKOGAWA, DA100) for pre-processing, and then are transmitted to a Pentium computer via a Multi-I/O interface for the calculation of the nondimensional parameter. As shown in Fig. 2, the entrance and two exits of the test section are respectively installed three pressure taps for the static-pressure-drop measurement. They are connected to a micro-differential transducer and a conditioner to amplifier the pressure signals which are subsequently transferred to a digital readout.

A total of eight trapezoidal ducts are tested in the present work. Two of them are smooth, cases A, and B; three are inserted with staggered pins (not an equilateral triangular array), cases C, E, and G; and the remaining three are inserted with in-line pins, cases D, F, and H. As for the duct outlet conditions, cases C to D have a single duct exit, while cases G and H have both exits in the straight and lateral directions. The ratio of lateral-to-total flow rate in cases G nad H varies from 0.2 to 0.8. Detailed configurations of the investigated pin-fin channels and associated parameters varied are provided by Fig. 3 (b) as well as Table 1.

DATA REDUCTION AND UNCERTAINTY

Heat Transfer Coefficient

The log-mean averaged heat transfer coefficient of the pin-fin channel is presented customarily in terms of the Nusselt number and is defined

$$\overline{Nu} = Q_c \bullet De / (A \bullet \Delta T_{lm} \bullet k_f) \tag{1}$$

where Q_c is the net heat transfer rate from the test section to the coolant, and is calculated by subtracting the heat loss from the supplied electrical power, i.e., $Q_c = Q_e - Q_l$. The electrical power generated from the foil heater is determined from the measured heater resistance and the current through the heater. It is also checked by measuring voltage drop across the heater. The total heat loss can be estimated by the following equation:

$$Q_l = Q_{bl} + Q_{sl} + Q_{al} \tag{2}$$

Q_{bl} represents the conduction loss from the backside of the heated plate to the environment, Q_{sl}, the lateral conduction loss through the two adiabatic side plates to the environment, and Q_{al}, the axial conduction loss through upstream and downstream ends of the heated plates. By using one-dimensional heat conduction analysis, they are estimated to be less than 6.0, 3.0, and 3.0 percents, respectively. To confirm energy conservation during the experiment, the total net heat transfer rate from the test duct to the cooling air is further checked with the cooling air enthalpy rise along the test duct, and a very good agreement is achieved. The log-mean temperature difference, ΔT_{lm}, in equation (1) is in terms of $\overline{T}_w$, T_{bi}, and T_{bo}, i.e.,

$$\Delta T_{lm} = \frac{\left(\overline{T}_w - T_{bi}\right) - \left(\overline{T}_w - T_{bo}\right)}{ln\left[\left(\overline{T}_w - \overline{T}_{bi}\right) / \left(\overline{T}_w - \overline{T}_{bo}\right)\right]} \tag{3}$$

The inlet bulk mean air temperature, T_{bi}, is measured by a thermocouple positioned at the test-section entrance, typically about 25-27℃. The wall temperature, $\overline{T}_w$, is an averaged value of the 14 thermocouple readings on the heated plate, and is read directly from the hybrid recorder. Note that since the end wall is made of highly conductive aluminum, the 14 thermocouples measure the average wall temperature rather than the local wall temperature. Therefore, in all test runs, the uniformity of the wall temperature is very well, with a maximum variation less than 2.2℃. To further check the temperature uniformity of the entire end wall, an additional thermocouple is

instrumented in the region near the remote corner where the heat transfer coefficients are expected to be localized. This temperature reading, however, is only 0.8℃ higher than the above average wall temperature. Therefore, we should recognize here that, by using the present test rig, only the average heat transfer coefficients could be obtained. In addition, since the total heat transfer area (A, including the end walls and the pin surfaces) is employed to determine the log-mean average heat transfer coefficients (Eq. (1)), the pin surface temperature should not be different too much from the end wall temperature. A simple calculation is done to check the validity of this assumption by using the heat transfer coefficients from a cylinder-in-crossflow correlation by Zhukauskas (1972). It is found that the maximum deviation of the temperature between the pin surface and the end wall is less than 3 %. The typical difference between the averaged wall temperature and the inlet air temperature is fixed 30±2℃ by adjusting the power input the heater. The common outlet bulk-mean air temperature based on the two streams, T_{bo}, is evaluated as

$$T_{bo} = (1-\varepsilon)\,T_{bs} + \varepsilon\,T_{bl} \tag{4}$$

where ε is the ratio of lateral-to-total flow rate. T_{bs} and T_{bl} are the bulk mean temperatures of the exiting air, and are respectively measured by three thermocouples positioned at the straight and lateral outlets of the test section. Also, by using an energy balance, the common outlet bulk mean air temperature can be readily calculated as $T_{bo} = T_{bi} + Q_c/(Gc_p)$. It is found that the agreement of T_{bo} obtained from these two methods is very good, typically within approximately 5 percent in discrepancy.

Pressure-Drop Coefficient

The pressure drop across the finite-length duct of trapezoidal cross section can be made dimensionless as

$$K_L = 2\,\Delta P/(G^2/\rho) \tag{5}$$

This non-dimensional pressure-drop parameter can be represented by multiplying the Darcy friction factor by the dimensionless length L/De, i.e.,

$$K_L = f \bullet (L/De) \tag{6}$$

The pressure-drop coefficient obtained is based on adiabatic conditions (i.e. test without heating).

Reynolds number

The Reynolds number used herein is based on the average velocity, i.e.,

$$Re = G \bullet De/\mu \tag{7}$$

where De is the equivalent hydraulic of the trapezoidal duct, i.e., $4A_c/(2W+H_1+H_2)$. This reduction is similar to that in VanFossen (1982), but is different from that in Mezeger et al. (1982) and Kumaran et al. (1991), in which the Reynolds number is based on the pin diameter and the maximum velocity in the duct. This is not peculiar because the overall heat transfer in trapezoidal ducts, either with or without pin-fin enhancement, is interesting in the present study; while the previous works were devoted to pin-fin heat transfer. The Reynolds number ranges from 6000 to 40000, which is similar to the range of interest for the turbine cooling application (VanFossen, 1982).

Uncertainty

The individual contributions to the uncertainties of the nondimensional parameters for each of the measured physical properties are summarized in Table 2. By using the estimation method of Kline and McClintock (1953), the maximum uncertainties of the investigated nondimensional parameters are as follows: Re, 6.5 %; $\overline{Nu}$, 8.4 %; and K_L, 7.6 %.

RESULTS AND DISCUSSION

Log-Mean Averaged Heat Transfer Coefficient

Smooth Duct. It is important to validate the present experimental procedure and results by comparing the present data with previous works. Figure 4 shows the comparison of overall heat transfer between the present smooth-trapezoidal-duct results and a correlation (dashed line, McAdam, 1954) of length-mean heat transfer for developing turbulent pipe flow. The circular and triangular symbols here pertain to the results of cases A and B, respectively (i.e., ducts with straight exit and lateral exit, respectively). Since the present trapezoidal test section has only about 3.7 times the duct hydraulic diameter in streamwise distance, the entrance-length effect on the overall heat transfer in this finite-length test section should be significant. To make the comparison fairly, the correlation selected in Fig. 4, which was modified from the Dittus-Boelter equation (Dittus and Bolter, 1930), has considered the entrance-length effect. It is observed from this figure that, within the range of Reynolds number investigated, the agreement between the modified correlation and the present experimental data of case A is very good. This good agreement gives confidence that the present measurement technique and the data analysis are working well. Further observing Fig. 4 has that the log-mean averaged Nusselt number for case B is higher than that for case A. The higher heat transfer for the lateral-outlet-flow duct may be attributed to the acceleration of coolant through the convergent lateral exit and, partly, the significant flow turning effects.

Effect of Outlet-flow Direction. Figures 5-7 show the overall heat transfer in the present trapezoidal ducts with pin arrays. Attention is first focused on Fig. 5 for the results that ducts have a single exit (i.e., cases C to F). In this figure, the log-mean averaged Nusselt numbers are shown as a function of Reynolds number. The corresponding smooth-walled results are also included for comparison. The symbols represent the actual experiments and the solid lines passing through these symbols are curve fits of the forms

$$\overline{Nu} = a\,Re^{b} \tag{8}$$

where the values of a and b are listed in Table 3. The maximum deviation between the equation above and the experimental data shown in Fig. 5 is less than 5 percent. From Fig. 5 and Table 3, the log-mean averaged Nusselt number in the pin-fin trapezoidal duct increases with increasing the Reynolds number. In the trapezoidal duct with straight

outlet flow, the staggered pin arrangement (case C) has higher overall heat transfer than the in-line pin arrangement (case D). Physically, heat transfer enhancement is favored by the more tortuous flow of a staggered arrangement (Incropera and DeWitt, 1994). As for the lateral-outlet-flow ducts (cases E and F), interestedly, the log-mean averaged heat transfer coefficient is insensitive to the pin arrangements investigated. This is very reasonable because, in these two cases, the main flow has to turn to the lateral exit totally; in such a way, the pin array for case F appears to be a staggered fashion to the turning flow. Therefore, with respect to the turning main flow, the pin arrangements for cases E and F do not differ from each other too much. It is further observed from this figure that, for both the staggered and the in-line fashions, the lateral-outlet-flow ducts (cases E and F) perform the better heat transfer coefficients than the corresponding straight-outlet-flow ducts (cases C and D). In comparison of the smooth-duct results with straight outlet flow (centerline), the enhancement in the overall heat transfer is up to about 120, 70, 160 and 160 percent for cases C, D, E, and F, respectively, in the range of Reynolds number investigated.

It is worthwhile to make a comparison of the log-mean averaged heat transfer coefficients in the present pin-fin trapezoidal duct and those in previous pin-fin rectangular ducts. The dashed line shown in Fig. 5 is the VanFossen correlation (VanFossen, 1982) for a straight-outlet-flow channel with staggered pin array. His data were obtained in a rectangular test section with four rows of copper and wooden short pins (l/d = 0.5, and 2.0); while the present data of case C are obtained in a trapezoidal duct with five rows of aluminum pins of an averaged pin length l/d = 2.0. Figure 5 shows that the present data of case C compare well with his correlation.

Effect of Lateral Flow Rate Ratio. The overall heat transfer in the trapezoidal ducts with straight as well as lateral exits (i.e., both exits are open) is shown in Figs. 6, and 7, respectively, for the staggered (case G) and in-line (case H) pin arrangements. Experimental data for the ratios of lateral-to-total flow rate (ε) from 0.2 to 0.8 are shown in these figures. For convenience, the results that pin-fin ducts have only a single exit (cases C to F, dashed lines) are also plotted on these figures. It is found in Figs. 6 and 7 that the log-mean averaged Nusselt number for the small lateral flow rates (ε = 0.2 and 0.4) is lower than that without lateral outlet flow (cases C and D). But at high lateral-flow conditions, say ε = 0.8, the $\overline{Nu}$ is higher than that without lateral outlet flow (cases C and D). The explanation of this fact is as follows. When both the straight exit and the lateral exit are open, the fluid either flows straight downstream or turns laterally; therefore the apparent cross-sectional area for the throughflow is higher than that with a single exit only. The increase in the duct cross-sectional area reduces the averaged throughflow velocity, hence overall heat transfer. However, further increasing the lateral flow rate ($\varepsilon \geq 0.6$ or 0.8) adds the effect of flow acceleration through the convergent lateral exit as well as the flow turning effect that, in turn, augments the overall heat transfer.

For clarity, the effect of the ratio of lateral-to-total flow rate on the log-mean averaged Nusselt number in trapezoidal ducts are further shown in Fig. 8 for a fixed Reynolds number of Re = 20,000. Results of the single-outlet ducts, i.e., cases C to F, are also provided for extrapolation. The symbols are actual experiments and the solid lines passing through these symbols are curve-fitting results. Both the staggered and the in-line pin configurations reveal a general trend, namely, the log-mean averaged Nusselt number starts with a decrease with increasing ε, then sharply increases with increasing ε after about $\varepsilon \geq 0.4$, and finally approaches a maximum value at ε = 1.0. The log-mean averaged heat transfer coefficient in the trapezoidal duct with staggered pin array has a local minimum at approximately ε = 0.3. However, for the in-line pin array, the rate of decrease in the log-mean averaged Nusselt number in the low ε range is not as much significant as that for the staggered pin array. This is because the in-line pin configuration looks like a staggered pin configuration relative to the turning flow, which positively enhances the log-mean averaged heat transfer. Consequently, the decrease in overall heat transfer due to the reduction in the throughflow velocity mentioned above is somewhat compensated by this effect. Another notable feature is that at high lateral flow conditions, say $\varepsilon \geq 0.8$, the log-mean averaged Nusselt number seems to be unaffected by the pin arrangement. The previous results in a rectangular pin-fin duct by Lau et al. (1989) are shown by a data band in this figure for comparison. Their data showed that the log-mean averaged Nusselt number is decreased monotonically with the increase in the ratio of lateral-to-total flow rate from ε = 0 to 1.0. The disagreement in the ε dependence of the log-mean averaged Nusselt number between the present and previous data may be due to the difference in the cross-sectional area of the test duct investigated. Further investigation is need to examine in detail the effect of ε on the heat transfer characteristics in ducts of different cross sections.

Pressure Drops

Smooth Duct. Figure 9 shows the overall pressure-drop coefficient of the present smooth trapezoidal ducts as a function of Reynolds number. Firstly, the present pressure-drop results for the trapezoidal duct with straight outlet flow (case A) are compared with the previous correlation (Petukhov, 1970) for the smooth pipe flow, and a good agreement is achieved. This comparison confirms again the reliability of the present data and the validation of the present experimental procedure. As for the trapezoidal duct with lateral exit (case B), physically, the flow in this situation is largely similar to that the fluid flows though a 90 deg sharp bend. Therefore, the previous results of pressure drop across a 90-deg miter with uniform cross section at duct entrance and exit (Munson, et al., 1994) is plotted for comparison. It is observed from this figure that the overall pressure-drop coefficients for case B are significantly higher than those in the straight-outlet-flow duct (case A), but lower than those across the 90-deg miter. This may be because case B results in the separated region of the flow near the concave corner formed between the longer side wall and the blocked straight exit, and the swirling secondary flow that occurs due to the imbalance of the centripetal forces as a result of the curvature of the duct centerline. The reason for the later fact may be explained as that in the present trapezoidal duct the convergence in the flow cross-sectional area from the duct entrance to the lateral exit reduces the pressure drops.

Pin-Fin Duct. The pressure drops across the present trapezoidal ducts with staggered and in-line pin arrays are shown in Fig. 10 as a function of Reynolds number. In this figure, the previous experimental results (Lau et al., 1989) for the straight-outlet-flow duct are also plotted for comparison. The results of Lau et al. (1989) were obtained from a 15:1 rectangular channel with 33 pins. The pin length-to-diameter ratio and pin spacing-to-diameter ratio were fixed at l/d = 1.0 and S_L/d = S_T/d = 2.5, respectively. The Reynolds number was developed in terms of the pin diameter and the maximum flow velocity in the duct in their work. Accordingly, the data of Lau et al. (1989)

shown in Fig. 10 have been recast for the common basis. It is seen that the present data of case C (circular symbols) are higher than Laus' data. This may be attributed to the taller pins employed in the present work. Qualitatively, the data of the present and previous works reveal that the overall pressure-drop coefficients are nearly independent on the Reynolds number and stay almost at a constant value as the Reynolds number varies. Similar trends were observed by several investigators (Metzger et al., 1982; Lau et al., 1989).

It is further shown in Fig. 10 that the pin-fin trapezoidal ducts with lateral exit (cases E and F) have much higher pressure-drop coefficients than those with straight exit (cases C. and D). Comparing to the results of the smooth duct with a straight outlet flow (case A), the pressure-drop coefficients are about 12 to 15-fold, and 3 to 5-fold, respectively, for the trapezoidal duct with lateral exit (cases E, and F) and that with straight exit (cases C and D). As for the effect of pin arrangement, the staggered pin array pays more pressure-drop penalties than the in-line pin array in the trapezoidal duct with straight exit. In the trapezoidal duct with lateral exit, however, the in-line and staggered pin arrays have almost the same overall pressure-drop coefficients.

CONCLUDING REMARKS

Overall heat transfer and pressure drop in pin-fin trapezoidal ducts, simulating the trailing edge cooling cavities of turbine blades, have been performed experimentally. This study has extended the rectangular-duct works originated by Metzger et al. (1982) and VanFosson (1982) to a more realistic geometry. In addition, the effect of the lateral-to-total flow rate ratio on heat transfer and pressure drop in a trapezoidal duct, which has not been considered before, has been examined. Main findings based on the experiment are:

(1) The log-mean averaged Nusselt number for the smooth trapezoidal duct with lateral exit (case B) is higher than that with straight exit (case A), which may be attributed to the acceleration of coolant through the convergent lateral exit as well as the significant flow turning effects for the lateral-outlet-flow case.

(2) In the trapezoidal duct with lateral exit only, the log-mean averaged Nusselt numbers for the in-line pin array are largely identical to those for the staggered pin array. This trend is different from that in the trapezoidal duct with straight outlet flow, in which the staggered pin array has higher heat transfer than the in-line pin array.

(3) For the duct with straight as well as lateral outlets, the effect of ε on the log-mean averaged Nusselt number in previous rectangular ducts is significantly different from that in the present trapezoidal ducts. In previous rectangular ducts, the log-mean averaged Nusselt number decreases monotonically with increasing ε. In the present trapezoidal duct, the staggered pin array has a local minimum log-mean averaged Nusselt number at about $\varepsilon = 0.3$, while the log-mean averaged Nusselt number is relatively unaltered before $\varepsilon \leqq 0.4$ for the in-line pin array. For both pin configurations, the log-mean averaged Nusselt number increases with increasing lateral flow rate ($\varepsilon \geqq 0.4$). After $\varepsilon \geqq 0.8$, the log-mean averaged Nusselt number is nearly independent of the pin configuration.

(4) As for the duct with a straight exit, the staggered pin array pays more pressure-drop penalty as compared with the in-line pin array. In the trapezoidal duct with a lateral exit, however, the in-line and staggered pin arrays have almost the same overall pressure-drop coefficients.

ACKNOWLEDGMENTS

This work was sponsored by the National Science Council of the Republic of China under contract No. NSC 85-2212-E-216-003.

REFERENCES

Brigham, B. A., and VanFossen, G. J., 1984, "Length to Diameter Ratio and Row Number Effects in Short Pin Fin Heat Transfer," *Trans ASME, J. Engineering for Gas Turbine and Power*, Vol. 106, pp.241-245.

Dittus, F. W., and Boelter, L. M. K., 1930, University of California at Berkeley, *Publicatians in Engineering*, Vol. 2, pp. 443.

Hwang, J. J., 1997, "Turbulent Heat Transfer and Fluid Flow a Porous-Baffled Channel," *AIAA, J. Thermaphysics and Heat Transfer*, Vol. 11, pp. 429-8436.

Incropera, F. P., and DeWitt, D. P., 1994, Introduction to Heat Transfer, 3rd Ed., John Willey & Sons, New York.

Kline, S. J. and McClintock, F. A., 1953, "Describing Uncertainties on Single-Sample Experiments," *Mechancal Engineering*, Vol. 75, pp.1953.

Kumaran, T. K., Han, J. C., and Lau, S. C., 1991, "Augmented Heat Transfer in a Pin Fin Channel with Short and Long Ejection Holes" *Int. J. Heat Mass Transfer*, Vol. 34, pp. 2617-2628.

Lau, S. C., Kim, Y. S., and Han, J. C., 1987, "Local Endwall Heat/Mass Transfer Distributions in Pin Fin Channels" *AIAA, J. Thermaphysics and Heat Transfer*, Vol. 1, pp. 365-372.

Lau, S. C., Han, J. C., and Kim Y. S., 1989, "Turbulent Heat Transfer and Friction in Pin Fin Channels with Lateral Flow Injection" *Trans. ASME, J. Heat Transfer*, Vol. 111, pp. 51-58.

McAdams, W. H., *Heat Transmission*, 3rd ed., McGraw-Hill, New York, 1954.

Metzger, D. E., Berry, R. A., and Bronson, J. P., 1982, "Developing Heat Transfer in Rectangular Ducts with Staggered Pin Fins," *Trans ASME, J. Heat Transfer*, Vol. 104, pp.700-706.

Metzger, D. E., and Haley, W. W., P., 1982, "Heat Transfer Experiments and Flow Visualization for Arrays of Short Pin Fins," *ASME Paper No. 82-GT-138*.

Metzger, D. E., Fan, C. S., and Haley, S. W., 1984, "Effects of Pin Shape and Array Orientation on Heat Transfer and Pressure Loss in Pin Fin Arrays," *Trans ASME, J. Heat Transfer*, Vol. 106, pp.252-257.

Munson, B. R., Young, D. F., and Okiishi, T. H., 1994, *Fundamentals of Fluid Mechanics*, 2nd ed., John Wiley & Sons, New York.

Petukhov, B. S., 1970, *Advances in Heat Transfer*, Vol.6, pp. 503-504, Academic, New York.

VanFossen, G. J., 1982, "Heat-Transfer Coefficients for Staggered Arrays of Short Pin Fins," *Trans ASME, J. Heat Transfer*, Vol. 104, pp.268-274.

Zhukauskas, A. 1972, "Heat Transfer From Tubes in Cross Flow," *Advances in Heat Transfer*, Vol. 8, Academic, New York.

Table 1 Test section configuration

Case	Pin Arrangement	Number of Pins	Straight Exit	Lateral Exit	ε
A	SMOOTH	0	OPEN	BLOCKED	0
B	SMOOTH	0	BLOCKED	OPEN	1.0
C	STAGGERED	5×5	OPEN	BLOCKED	0
D	IN LINE	5×5	OPEN	BLOCKED	0
E	STAGGERED	5×5	BLOCKED	OPEN	1.0
F	IN LINE	5×5	BLOCKED	OPEN	1.0
G	STAGGERED	5×5	OPEN	OPEN	0.2-0.8
H	IN LINE	5×5	OPEN	OPEN	0.2-0.8

Table 2 Typical nondimensional interval for the relevant variables

Variables	Uncertainty
Air density, ρ	± 1.3 %
Specific heat of air, c_p	± 3.0 %
Dynamic viscosity of air, ν	± 2.9 %
Air thermal conductivity, k_f	± 1.5 %
Equivalent duct hydraulic diameter, De	± 0.5 %
Air mass flux, G	± 5.4 %
Log-mean temperature difference, ΔT_{lm}	± 3.0 %
Net heat flux, Q_c	± 7.6 %
Pressure difference, ΔP	± 5.1 %

Table 3 Coefficients and exponents of heat transfer correlation

CASE	$\overline{Nu} = a\,Re^b$	
	a	b
C	0.188	0.662
D	0.118	0.690
E	0.254	0.651
F	0.288	0.636

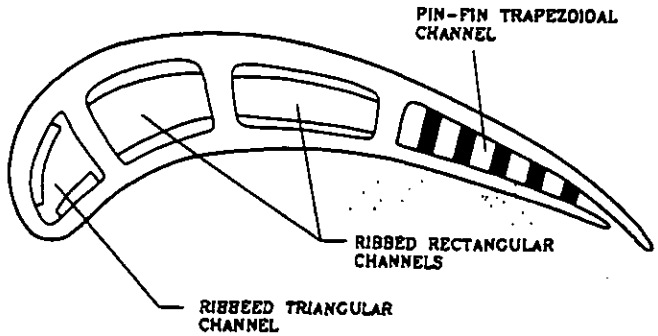

Figure 1 Cross-sectional view of the modern internally cooled turbine blade.

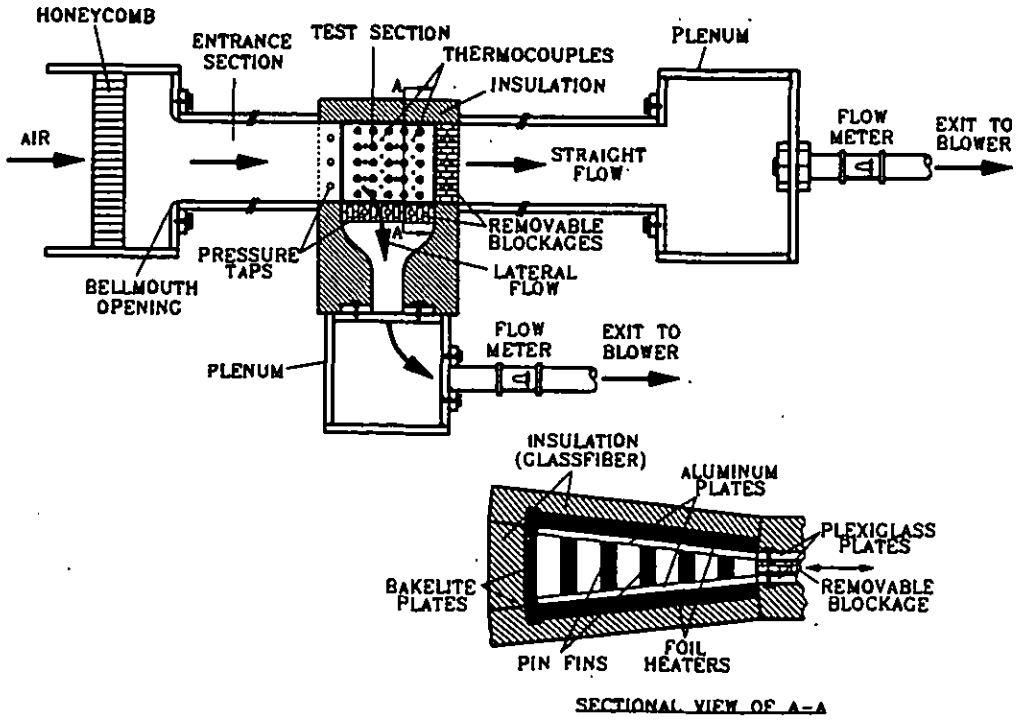

Figure 2 Sketch of the experimental apparatus, and the construction of the test section.

UNIT:mm

W	L	S_L	S_T	H_1	H_2	d
160	160	30	30	48	12	12

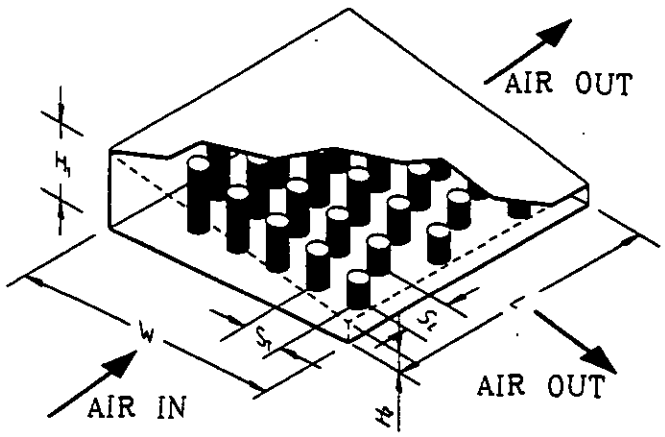

Figure 3 (a) Dimensions of the pin-fin trapezoidal duct investigated.

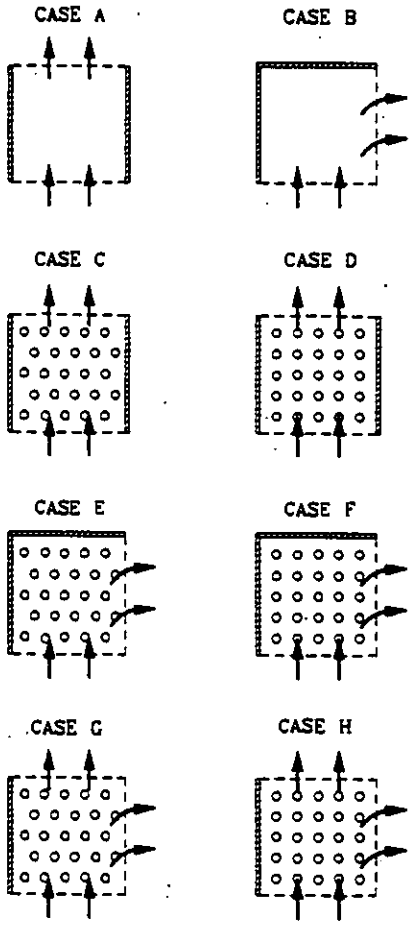

Figure 3 (b) Schematic of top view of pin-fin channels from cases A to H.

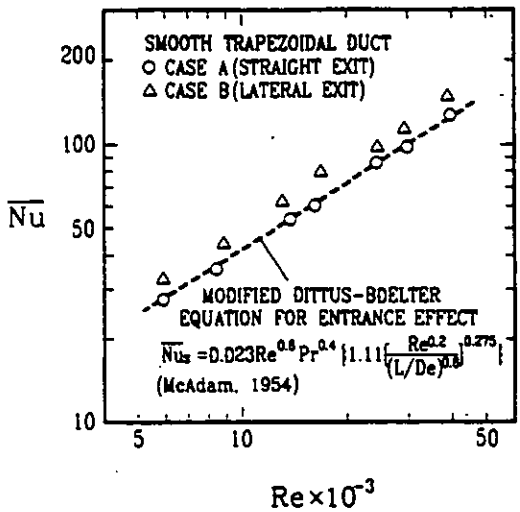

Figure 4 Comparison of average heat transfer of the present smooth trapezoidal duct and the previous correlation.

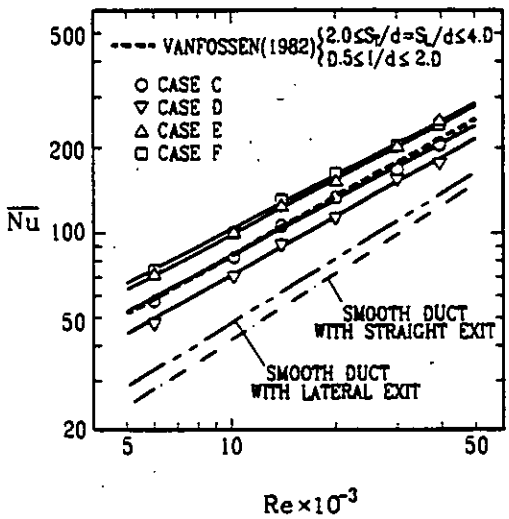

Figure 5 Reynolds number dependence of log-mean averaged Nusselt number for cases C to F.

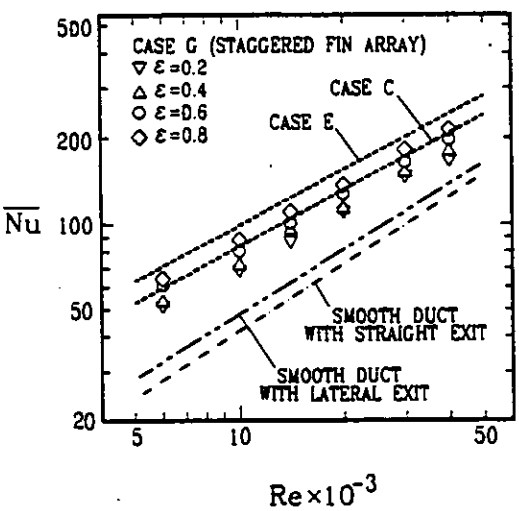

Figure 6 Reynolds number dependence of log-mean averaged Nusselt number for case G.

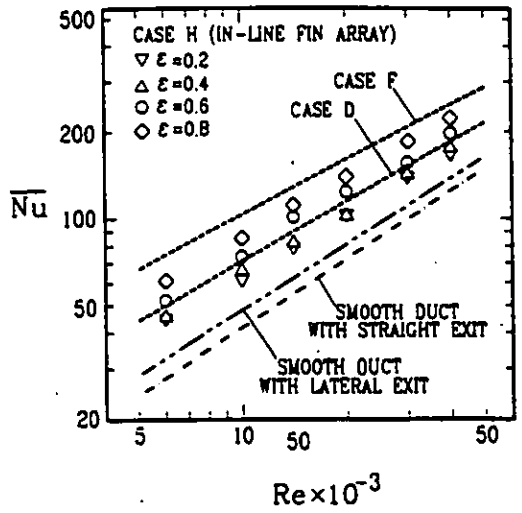

Figure 7 Reynolds number dependence of log-mean averaged Nusselt number for case H.

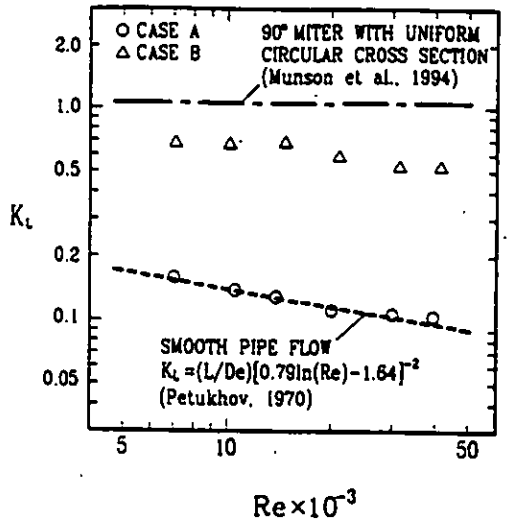

Figure 9 Comparison of overall friction coefficient present smooth trapezoidal ducts with previous correlation.

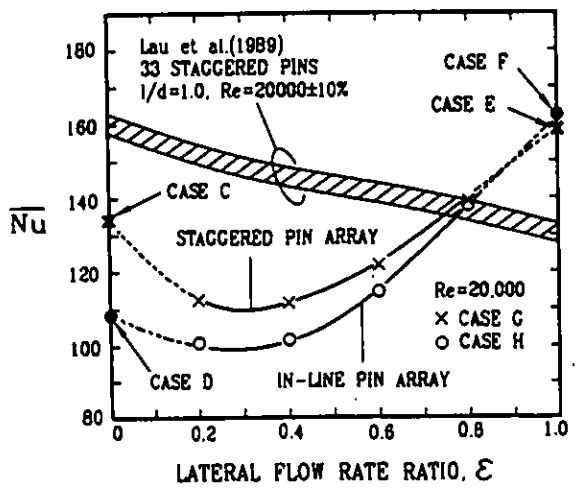

Figure 8 Effect of the ratio of lateral-to-total flow rate on log-mean averaged Nusselt number for staggered and in-line pin arrays.

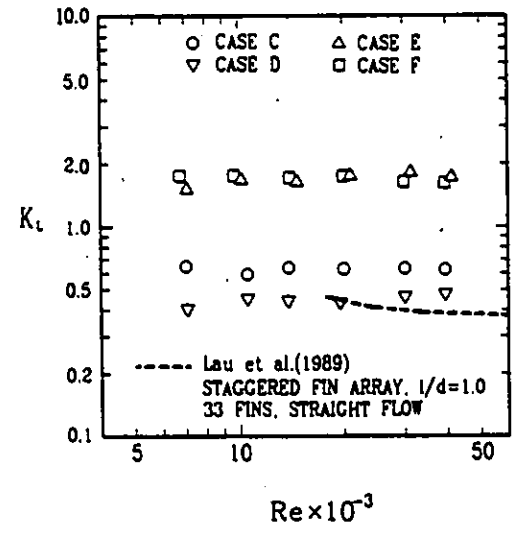

Figure 10 Reynolds number dependence of overall pressure-drop coefficient of the present pin-fin trapezoidal ducts for cases C to F.